RSC Applied Interfaces

ROYAL SOCIETY OF CHEMISTRY

PAPER

View Article Online
View Journal | View Issue

Cite this: *RSC Appl. Interfaces*, 2025, **2**, 1359

Accessing the corrosion resistance for metallic surfaces using long-chain fatty acids†

Sapan Kumar Pandit, Kushal Yadav, Poonam Chauhan and Aditya Kumar *

Received 30th April 2025,
Accepted 16th May 2025

DOI: 10.1039/d5lf00125k

rsc.li/RSCApplInter

In this study, the corrosion resistance of a metallic surface is provided by a superhydrophobic coating, which can protect it from dirt and water. The aluminium surfaces are modified with different long-chain fatty acids using a simple immersion technique. The modified aluminium surfaces exhibit excellent water-repellent properties with a static water contact angle of more than 150° and a sliding angle of less than 10°. The corrosion resistance of the modified surfaces was measured using a potentiodynamic technique in a 3.5% (w/v) NaCl solution. The Tafel plot shows an enhancement in corrosion resistance with a low corrosion current density and high corrosion potential after modification. The highest E_{corr} value of −0.7819 V and the lowest corrosion current density of 1.48×10^{-6} A cm^{-2} are found to be for the octadecanoic acid coated sample. Furthermore, the rate of corrosion resistance is analysed based on the length of fatty acids. Additionally, the modified aluminium surface also shows a dirt-resistant nature. The performance of the coated surface was investigated under several operating conditions including elevated temperature, contact with highly acidic and alkaline solutions, and different mechanical tests (surface bending, water jet, tape-peeling, and abrasion using sandpaper), which fulfils the industrial suitability of aluminium after modification.

1. Introduction

Aluminium is known for its unique properties such as good thermal and electrical conductivities, high specific strength, ductility, malleability, and light weight. It is widely used in several industrial and household applications including aircraft, automobile parts, packaging, powerlines, shipping, kitchen wares, and national defenses.[1] In an atmospheric environment, aluminium remains resistant to corrosion due to the presence of an inherent native oxide layer, which prevents the oxidation of the surface. However, it undergoes corrosion in water and constant contact with moisture.[2] Corrosion makes it vulnerable to further deterioration and leads to permanent failure of the system. Therefore, it is necessary to modify the surface to combat the above problem. Water or dirt are the main causes of corrosion on metal surfaces due to the tendency to lose the electron to oxygen in water so if the aluminium surface is water-repellent or has poor wettability, the corrosion resistance can be increased. The concept of 'wettability' refers to how a solid surface interacts with water and its ability to absorb or repel the water. High wettability signifies that a surface quickly absorbs water, whereas low wettability implies that it does not absorb water. In this context, the water contact angle is used to measure the wettability of any surface. High wettability reveals a low water contact angle, signifying a strong affinity for water. Meanwhile, low wettability results in a high water contact angle, indicating resistance to water interaction with the surface. Consequently, a direct correlation exists between the water contact angle and corrosion resistance. A higher water contact angle indicates greater corrosion resistance. Therefore, a protective layer of water-repellent nature or high-water contact angle (*i.e.*, hydrophobic or superhydrophobic) has shown great capabilities for controlling the corrosion rate.

Superhydrophobicity is defined as a water droplet with a water contact angle of more than 150° and negligible contact angle hysteresis.[3] Due to the low adhesion between the droplet and the surface, the droplet exhibits a spherical shape and easily rolls from the surface without wetting it. These superhydrophobic and hydrophobic surfaces have shown great potential for reducing corrosion by maintaining no contact with water. In nature, many fascinating examples exist such as lotus leaves, cicada wings, legs of water striders, pond skaters, and wings of butterflies,[4–8] which are known for their excellent superhydrophobic properties. These naturally gifted superhydrophobic materials exhibit excellent water repellency due to the presence of nano/micro rough structures on their surface and low surface energy. Therefore, to enhance the corrosion resistance of aluminium, lab-scale

Department of Chemical Engineering, Indian Institute of Technology (Indian School of Mines) Dhanbad, Jharkhand, 826004, India. E-mail: adityaku43@gmail.com

† Electronic supplementary information (ESI) available. See DOI: https://doi.org/10.1039/d5lf00125k

superhydrophobicity can be created by the combination of nano-microstructures and surface modification with low surface energy materials.

In general, on the lab scale surface roughness can be created by various methods like chemical etching,[9] lithography,[10] sandblasting,[11] 3D printing,[12] embedding the nanoparticles or microparticles and electrochemical deposition.[9] Among the above methods, chemical etching is the easiest method for creating roughness because lithography, sandblasting, and 3D printing are quite long processes along with high cost, and nanoparticles embedded on the metal surface can be easily removed by some mechanical forces. Particularly for metals, chemical etching can easily generate micro/nano-structures because the chemical etchant attacks the defects present on the surface.

Recently, researchers have been actively studying superhydrophobic coatings on aluminium surfaces to protect them from corrosion. For example, Tudu *et al.*[13] created anticorrosive superhydrophobic aluminium *via* chemical etching using sodium hydroxide (NaOH) followed by immersion in hexadecyltrimethoxysilane (HDTMS). Wang *et al.* developed a corrosion-resistant superhydrophobic aluminium *via* spray coating techniques using fluorinated ethylene polypropylene, polydimethylsiloxane, and polyphenylene sulfide.[14] Chen *et al.* prepared corrosion-resistant superhydrophobic coating on aluminium surfaces using hydrochloric acid (HCl) as an etchant and modified the surface with stearic acid.[15] Varshney *et al.* obtained a superhydrophobic aluminium surface by chemical etching with potassium hydroxide (KOH) followed by immersion in an ethanol solution of lauric acid.[16] Rasitha *et al.* optimized coating parameters for the fabrication of robust superhydrophobic (SHP) aluminium and evaluated its corrosion performance in an aggressive medium *via* a chemical etching process using a hydrochloric acid solution.[17] Peng *et al.* synthesized a corrosion-resistant superhydrophobic aluminium alloy using the chemical etching technique with chemical etchant and further modification with organic carbon dots.[18] Shuwei *et al.* fabricated superhydrophobic aluminium using octadecanethiol ($C_{18}H_{38}S$) to control corrosion. In this work, to generate a rough structure, chemical etching processes are used such as acid pickling and zinc immersion.[19] Zhang *et al.* fabricated a superhydrophobic aluminium surface using hydrochloric and myristic acid.[20] Rodic *et al.* developed superhydrophobic coating on the aluminium substrate by a chemical etching process using iron chloride ($FeCl_3$) solution and then immersion in an ethanol solution containing perfluorodecyltriethoxysilane.[21] Feng *et al.* developed a superhydrophobic aluminium surface after treatment in boiling water and modified it with stearic acid. The superhydrophobic surface presented a WCA ~154° with excellent corrosion resistance properties.[22]

Besides the surface roughness, the substrate needs to be modified by low surface energy materials such as fatty acids, chlorine or fluorine-based silanes, polymers, silicon–carbon, and hydrocarbon. Hydrogen chloride fumes that are poisonous and corrosive are produced when chlorosilanes combine with water, wet air, and steam. Gaseous hydrogen chloride may emit explosive and combustible gaseous hydrogen when it comes into contact with metals.[23] It is well recognized that the usage of fluorine-based compounds increases the danger of environmental contamination, human health issues such as hormonal imbalances, immunological disorders, and incurable diseases like thyroid disease, cancer, and Alzheimer's syndrome.[24] Polymer coatings are not resistant to abrasion and silicon–carbon materials are costly. Among all these chemicals, fatty acids are the most affordable and environmentally acceptable. If the carbon chain contains any acidic functional group, then it is a fatty acid. These fatty acids are divided into three groups namely short, medium, and long-chain fatty acids depending on the amount of carbon in the chain. The short chain contains 2–4 carbon atoms, and the medium chain consists of 6–10 carbon atoms. Whereas, long-chain fatty acids comprise 12–26 carbon atoms.[25]

In contrast to most studies that employ a single fatty acid or require complex multi-step fabrication, this work provides a systematic and comparative evaluation of three different long-chain fatty acids (dodecanoic ($C_{12}H_{24}O_2$), tetradecanoic ($C_{14}H_{28}O_2$), and octadecanoic acid ($C_{18}H_{36}O_2$)) on aluminium surfaces. By correlating superhydrophobicity with mechanical durability, thermal stability, and corrosion resistance, this study offers deeper mechanistic insights into eco-friendly surface modifications. Furthermore, the use of a simple immersion method, cost-effective materials, and detailed performance analyses under practical stress conditions demonstrates the strong potential for industrial scalability and real-world applications. These aspects distinctly position this work beyond conventional non-fluorinated superhydrophobic coatings reported over the last decade.

2. Experimental details

2.1 Materials requirement

An aluminium sheet (AA 6061) of thickness 1 mm was procured from Dhanbad Aluminium and Glass Pvt. Ltd. Sodium hydroxide (NaOH), ethanol, and acetone were purchased from Merck Specialties Pvt. Ltd., India. Dodecanoic acid (lauric acid), tetradecanoic acid (myristic acid), octadecanoic acid (stearic acid), and sodium chloride (NaCl) were procured from SRL Pvt. Ltd. Hydrochloric acid (HCl; 37 wt%) was purchased from Merck Life Science Private Ltd. All the chemicals were used as obtained without any further processing.

2.2 Sample preparation

The aluminium samples were taken with dimensions of 50 mm × 20 mm. Before coating, the aluminium substrates were sonicated in acetone for 60 min to remove any kind of impurities present on the surface. The cleaned aluminium substrates were then etched with 1 (w/v) % of NaOH solution

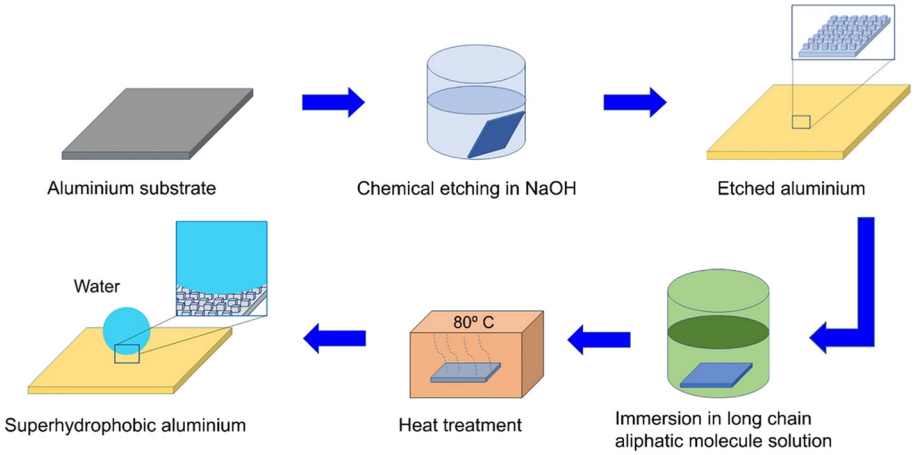

Fig. 1 Schematic diagram for the preparation of the superhydrophobic aluminium surface using long-chain fatty acids by a simple immersion technique.

in water for about 60 min as shown in Fig. 1. The optimization time for etching is taken based on previously optimized data by Lomga, J. *et al.*[26] The aluminium substrates after etching were cleaned in distilled water followed by acetone. The etched aluminium samples were then dried in an oven at 60 °C for 60 min. Three different solutions of aliphatic molecules (dodecanoic, tetradecanoic, and octadecanoic acid) were prepared in ethanol with a concentration of 4 (w/v) %. The solutions were prepared by mixing with a magnetic stirrer for 30 min each. The etched aluminium samples were then immersed in the above long chain aliphatic solutions for 24 h. Further, the fatty acid-coated samples were removed from the solutions and heated at 80 °C in an oven for 2 h each. To check the thermal effect on the metal substrate while depositing fatty acid-coating, the weight and the dimension of the samples were manually examined before and after coating. No change has been noticed in the aluminium sample due to the coating process.

2.3 Characterization

The surface morphology of the sample was examined with a field emission scanning electron microscope (FESEM, Supra55 Carl Zeiss, Germany). The water static contact angles and tilt angles were measured with a 3–5 μL volume of deionized water droplets using a drop shape analyzer (DSA25, Krüss Optronics, Germany) at ambient temperature. Contact angles were measured at five different places on each sample and their mean value was calculated. For tilt angle measurements, the sample was placed over the instrument's platform. Further, the water droplet was kept on the sample surface, and then the platform carrying the sample was tilted at certain angles. The tilt angle was measured at that point when the water droplet started to roll off from its surface. To study the presence of functional groups at the surface of coated samples, Fourier transform infrared spectroscopy (FTIR, Cary 660 FTIR, Agilent Technologies, USA) was used. To demonstrate the water-repellent characteristics, a floatation test was carried out. In the floatation test, the coated and uncoated samples were kept on the surface of the water and their behavior was recorded.

Mechanical, chemical, and thermal stability tests were conducted following well-established literature protocols. The chemical stability of the prepared coating was tested by immersing the coated samples in different pH solutions such as pH = 2 (HCl), pH = 3 (HCl), pH = 7 (tap water), pH = 8 (sea water), pH = 11 (NaOH), and pH = 13 (NaOH) and measuring the water contact angles at regular intervals of immersion. The thermal stability test was performed for 2 h exposing the samples to different annealing temperatures ranging from 50 to 300 °C. Mechanical durability was examined by tape peeling, sandpaper abrasion, water jet impact, and bending tests. The tape peeling test was performed by gluing one-sided insulation tape (electrical PVC, adhesion to aluminum: 1.3 to 2.2 N cm^{-1}) on the coated surface and then removing it. The contact angle was measured after each cycle of tape peeling (gluing and ungluing). The sandpaper abrasion test used 180 grit paper under a constant applied load of 0.2 N. The sample was moved manually at a speed of approximately 2 cm s^{-1} over a distance of 10 cm per abrasion cycle, and the water contact angle was measured after every cycle of the test. In the water jet test, a water jet (speed = 6.5 m s^{-1}, angle = 45°, distance = 4 cm) was sprayed from the syringe and the interaction of water with the coated and uncoated samples was studied. The bending test was conducted by repeatedly folding and unfolding the coated surface, covering an angle of approximately 160° in total. and measuring the water contact angle at the bent area of the coated sample.

A self-cleaning test was performed by contaminating the uncoated and coated samples with dust particles (chalk powder, particle size <30 micrometers) and then dropping the water droplets on the contaminated surfaces. The contaminated samples were positioned at a 30° inclination

to facilitate the movement of water droplets. And later the flow of water droplets was observed. A corrosion test was performed using a potentiostat (Booster10A, Metrohm Autolab B.V. Netherland). The measurements were made in a three-electrode cell system consisting of an Ag/AgCl as the reference electrode (conc. ~3 M KCl), a tested sample as the working electrode, and a platinum wire as the counter electrode. The Ag/AgCl reference electrode was calibrated against a saturated KCl solution before measurements. The exposed area of the working electrode was calculated to be approximately about 1 cm^2. The scan rate was 0.1 mV s^{-1} and the applied potential was set in the range of −0.1 V to +0.1 V. The experiment was carried out in 3.5 sodium chloride (NaCl, w/v%) solution after 30 min immersion of the working sample at room temperature. Polarization parameters such as corrosion current density, self-corrosion potential, and polarization resistance was derived from potentiodynamic curves. Higher corrosion potential and lower passivation current typically indicate superior corrosion resistance.

3. Results and discussion

In this work, water-repellent (superhydrophobic) modification on the aluminium surface was done by using three different long-chain fatty acids namely dodecanoic, tetradecanoic, and octadecanoic acids. To check the performance of the fabricated coating, chemical, mechanical, and thermal stability tests were done. Wettability, morphology, functionality, and a deep corrosion study along with the self-cleaning behavior were further conducted.

3.1 Wettability and surface morphologies

The wettability of the uncoated and coated aluminum surfaces were measured in term of static water contact angle. The static water contact angle of the uncoated aluminum surface was found to be 68 ± 3°, which shows the hydrophilic nature of aluminum. After etching, crater-like structures are formed on the aluminium surface, and the wetting property aluminium sample changed to superhydrophilic with a water contact angle of 6 ± 2°. After etching, the samples were

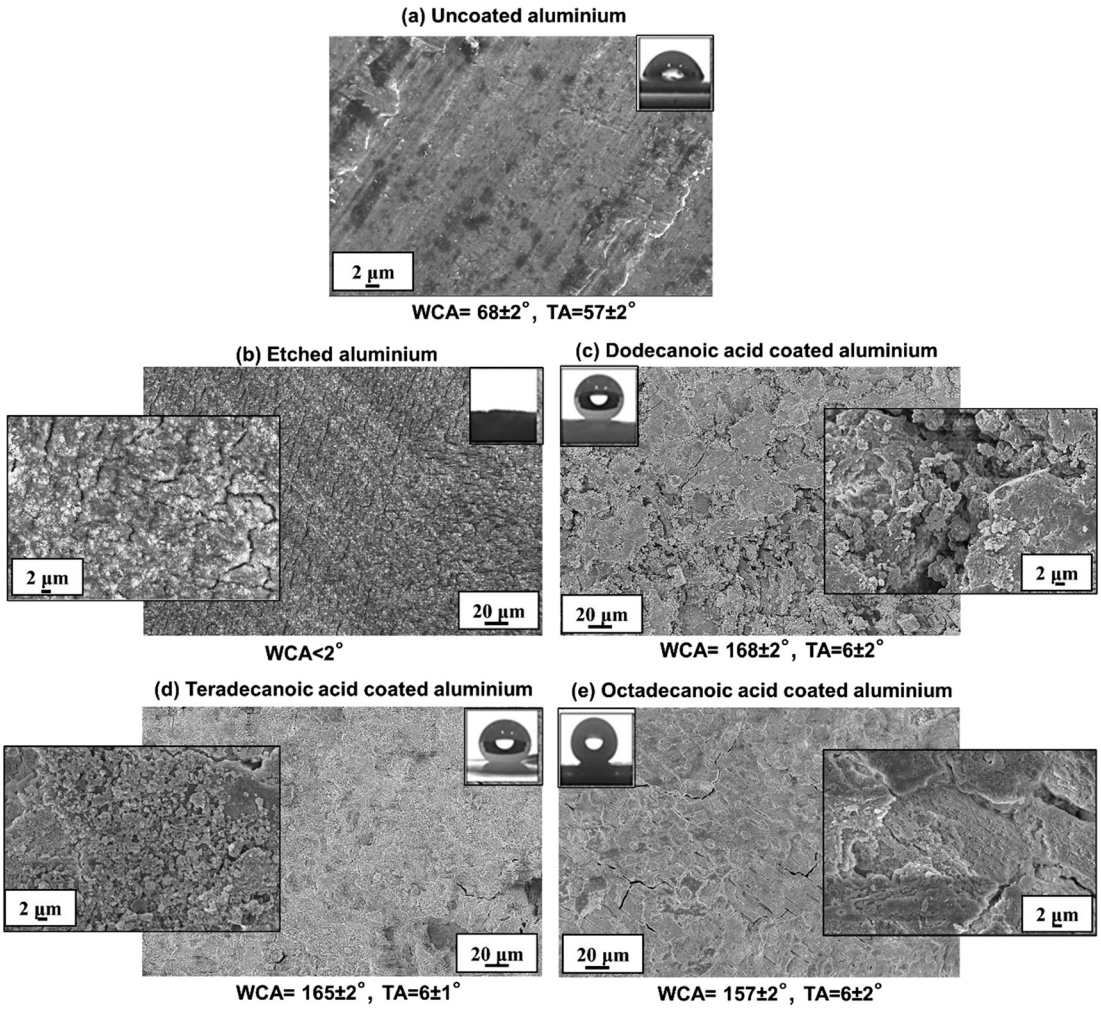

Fig. 2 SEM images of (a) uncoated aluminium, (b) etched aluminium with NaOH, (c) dodecanoic acid coated aluminium, (d) tetradecanoic acid coated aluminium, and (e) octadecanoic acid coated aluminium. The right-inserted images show the highly magnified image. The left-inserted images show the water contact angle images.

immersed in a fatty acid solution to modify them from hydrophilic to superhydrophobic. The modified aluminium surfaces exhibited an increased static water contact angle and a decreased tilt angle. Static water contact angles of 168 ± 2° after modification with dodecanoic acid, 165 ± 3° after modification with tetradecanoic acid, and 157 ± 2° after modification with octadecanoic acid were found. The tilt angles were 6 ± 2°, 6 ± 1°, and 6 ± 2° for dodecanoic acid, tetradecanoic acid and octadecanoic acid, respectively. This shows the successful achievement of superhydrophobicity after modification of aluminium with fatty acids.

To study the detailed mechanism of superhydrophobic aluminium formation, the surface morphologies of the coated and uncoated aluminium were investigated using SEM. The SEM images of the uncoated and coated samples are shown in Fig. 2. The images show the plane and smooth surface morphology of the uncoated aluminium with no complex structures, as shown in Fig. 2a. Etching is necessary for converting a hydrophilic surface into a superhydrophobic surface. The regular pits and craters are observed in etched aluminium help the surface change by creating air holes. After etching with NaOH for 60 min, a homogeneous surface with regular pits and craters was obtained (Fig. 2b).

During the etching process, the reaction taking place on the aluminium surface may be represented as

$$2Al\ (s) + 2NaOH(aq) + 6H_2O \rightarrow 2Na[Al(OH)_4](aq) + 3H_2(g) \quad (1)$$

$$Al_2O_3\ (s) + 2NaOH(aq) + 3H_2O \rightarrow 2Na[Al(OH)_4](aq) \quad (2)$$

$$Na[Al(OH)_4] \rightarrow NaAlO_2 + 2H_2O \quad (3)$$

$$NaAlO_2 + 2H_2O \rightarrow Al(OH)_3 + NaOH \quad (4)$$

Sodium hydroxide (NaOH) reacts with the aluminium surface during etching, which is typically carried out at room temperature, to create sodium aluminate, as demonstrated by reaction (1). In this reaction, OH^- ions in NaOH solution attack aluminium and form hydrated sodium aluminate ($Na[Al(OH)_4]$), which is responsible for etching the aluminium surface.[27] During the etching process, some bubbles are released, which are basically the by-product H_2 gas. Similarly, as mentioned in reaction (2), the dissolution of aluminium oxide occurs with sodium hydroxide and produces hydrated sodium aluminate. Despite having a stable native oxide layer that may prevent consistent etching from occurring on the aluminium surface, it allows the aluminium to be etched. Consequently, a high density of pit nucleation sites appeared on the aluminium surface. This facilitates the uniform etching of the aluminium surface due to the dissociation of excess sodium aluminate as per reaction (3).[26] Because of the continuous process, the sodium aluminate hydrolysis reaction takes place and produces $Al(OH)_3$ and NaOH as represented in reaction (4).

The etched aluminium samples were then immersed in ethanol and various long-chain fatty acid solutions. A morphological layer of long-chain fatty acids was deposited on the surface. The dehydration reaction takes place on the surface of aluminium, in which the carboxyl groups of different chain-length molecules react with the hydroxyl group on aluminium as shown in Fig. 3. Attached fatty acids form hydrophobic tails on the surface which can be represented as:

$$3R\text{–}COO^- + Al^{3+} \rightarrow Al(R\text{–}COO)_3 \quad (5)$$

After treatment with fatty acids the aluminium surface exhibited various features. This occurs because of treatment with an ethanolic solution of fatty acid, Al^{3+} ions are activated on the surface and react with the functional group of the fatty acid ($R\text{–}COO^-$), resulting in a monolayer of $Al(R\text{–}COO)_3$ on the aluminium surface. Moreover, the presence of free Al^{3+} ions were also observed. These free Al^{3+} ions further react with $R\text{–}COO^-$ and produce $Al(R\text{–}COO)_3$ molecules, which are later precipitated on the aluminium surface and form spongy spots. In the present study, we used three different fatty acids; therefore, spongy spots of different sizes and shapes were expected in all three-coated samples. The dodecanoic acid-coated surface exhibited a sponge-like morphology, as shown in Fig. 2c. In the case of tetradecanoic acid, the coating appeared very compact with minor crests and dips as shown in Fig. 2d.[28] On the other hand, the octadecanoic acid-coated surface also shows an intact layer with minor irregularities on the surface, as shown in Fig. 2e.[29] This occurs as a result of the dehydration process when the carboxyl at the positive end of the fatty acid combines with the hydroxyl or aluminium atom. A low surface energy aluminium surface was produced by bonding the long non-positive end of the alkyl to the etched aluminium surface. This makes it easier to increase the

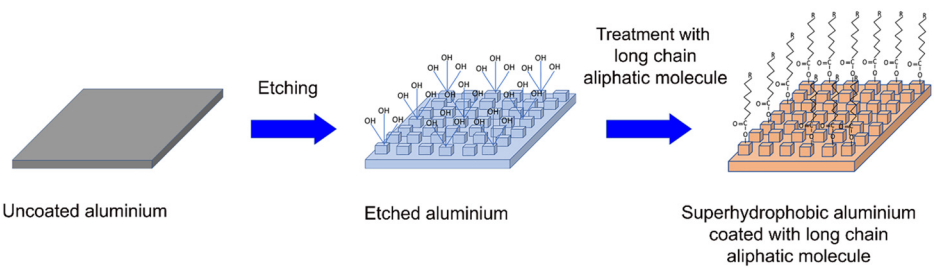

Fig. 3 Schematic representation of the reaction mechanism on the aluminium substrate after etching and testing by aliphatic molecules.

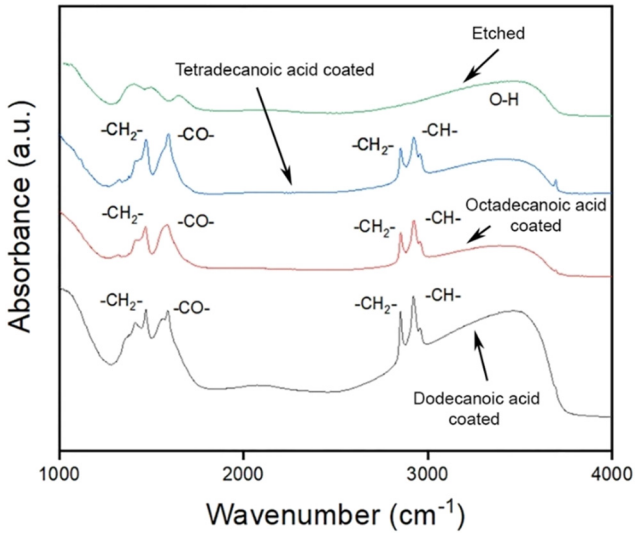

Fig. 4 FTIR spectra of etched aluminium and modified aluminium by aliphatic molecules.

contact angle from 68 ± 3° for uncoated aluminium to 168 ± 2° after modification.

FTIR analysis was performed to inspect the presence of functional groups on aluminium surfaces. The FTIR spectra of the three samples coated with dodecanoic acid, tetradecanoic acid, and octadecanoic acid are shown in Fig. 4. Four absorption peaks were observed in the case of each aliphatic molecule-coated surface. The peak observed at 1470 cm^{-1} in the case of dodecanoic acid-coated aluminium represents the symmetric stretching of the COO^- the coordinated group. Whereas the peaks at 2923 cm^{-1}, 2957 cm^{-1}, and 3380 cm^{-1} represent the asymmetric stretching of the C–H bond, C–H stretching in the CH_3– group, and stretching vibrations of the O–H bond, respectively. Similar peaks were observed in for tetradecanoic and octadecanoic acid-coated samples. In the case of tetradecanoic acid-coated surface, peaks at 3394 cm^{-1}, 2924 cm^{-1}, and 1468 cm^{-1} represent the O–H bond stretching band, C–H bond asymmetric stretching, and COO^- coordinated groups, respectively. The surface modified by octadecanoic acid showed a vast O–H stretching band at 3459 cm^{-1}, asymmetric stretching of the C–H bond at 2921 cm^{-1}, and COO^- coordinated group at 1468 cm^{-1}. The COO^- coordinated bonds at 1470 cm^{-1} clearly explain the reaction mechanism, as discussed above.

According to the Cassie–Baxter model, a rough surface is impermeable to liquid droplets. Instead, droplets sit atop at the ragged structures of the surface, trapping air beneath them. Smaller-scale features must be placed on top of bigger-scale features in order to create the Cassie–Baxter effect. In this work, SEM images of the etched samples show the ragged structure of the aluminium surface, which is responsible for trapping air beneath them. On the other hand, FTIR analysis confirmed the presence of hydrophobic tails of fatty acids, which is responsible for lowering the surface energy of aluminium. The combination of these results fulfils the criteria for becoming a superhydrophobic surface. Although octadecanoic acid (C18) has the longest chain length and its static water contact angle is lower than that of dodecanoic acid (C12), this is likely due to differences in packing density. At lower packing densities, longer alkyl chains tend to enhance surface roughness and exhibit greater flexibility, both of which contribute to increased hydrophobicity. In contrast, at higher packing densities, longer chains can lead to more ordered and rigid structures, which slightly diminishes the hydrophobic character due to reduced surface roughness and mobility.[30]

3.2 Wetting sustainability under harsh conditions

Metallic surfaces are generally exposed to mechanical, thermal, and chemical contacts. The pressure and impact of various contained third bodies also affect their morphology and surface properties. Therefore, there is a high chance of the wetting properties of these undergoing contacts being lost. The mechanical durability of the coatings was thus evaluated using tape peeling, water jet impact, surface bending, and sandpaper abrasion tests. To examine the adhesive behavior of the coating, a tape-peeling test was performed. The adhesive tape peeling test process is shown in Fig. 5a. In this method, an insulation tape is glued on the surface by ensuring that there are no air bubbles and the tape completely covers the surface.[13] The tape was then removed from the surface and the water contact angle was measured to ensure the wetting property. This process was continued until there is a complete loss of superhydrophobicity. Three sets of experiments were carried out to obtain the WCA values corresponding to the tape peeling cycles, as listed in Table 1. The variation between the water contact angles and peeling cycles for all coated surfaces is shown in Fig. 5b. In the case of dodecanoic acid, superhydrophobicity is lost after the 5th cycle of tape peeling and the water contact angle reduced to 148 ± 2°. In contrast, for the tetradecanoic acid coated sample, the superhydrophobicity remained unchanged up to the 10th cycle of tape peeling and the contact angle was found to be 145 ± 2° after the 10th cycle. Whereas, the octadecanoic acid-coated sample remained superhydrophobic until three cycles of tape peeling and the contact angle was 147 ± 2° after three cycles. The coating is damaged as a result of the mechanical force applied during the gluing and ungluing process of the tape. A similar observation was reported by Tudu *et al.*[13] These results further show that tetradecanoic acid has better durability due to the better packing of the molecules, however, this property also wears out after several repetitions of the tape-peeling cycle.

Furthermore, a bending test was performed to evaluate the effect of disturbances on the surface wettability.[27] The coated aluminium samples were folded and unfolded several times, and the contact angle was checked at the kinked area of the folded portion as shown in Fig. 6a. It is observed that

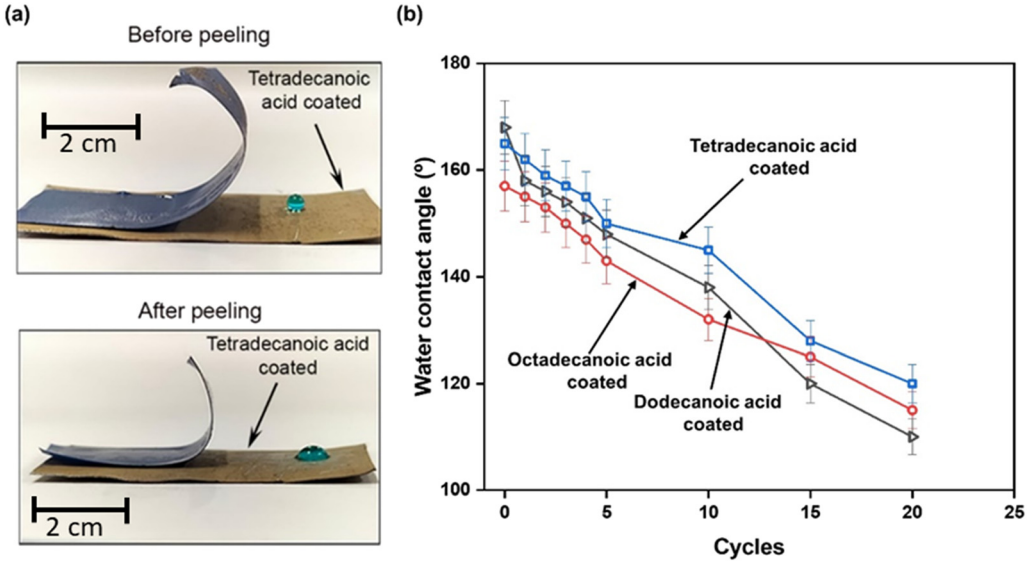

Fig. 5 (a) Optical images of an adhesive tape peeling test cycle for examining the adhesive strength durability of superhydrophobic coatings. (b) The plot between WCA and peeling cycles for coated surfaces.

superhydrophobicity remained unaltered for up to 15 cycles in the case of dodecanoic acid. In the case of tetradecanoic and octadecanoic acid-coated samples, the number of cycles was 17 and 20, respectively. The wettability of the coated surfaces remained undisturbed by the bending test up to the number of cycles mentioned above. The WCA of the octadecanoic acid-coated samples after 20 bending cycles was 143 ± 1°. Similar results have been observed in the previous study by Varshney *et al.*[27] It is possible that repeated bending of the coated aluminium samples can damage the coating by disrupting its micro-rough structure.

In the floating test, the water-repellent nature of the coated and uncoated samples was examined by floating them in water, as shown in Fig. 6b. The uncoated sample immediately sank to the bottom when it was kept on the surface of the water. Whereas, the superhydrophobic aluminium floats on the surface of the water, which reveals its excellent water-repellent characteristics. Aluminium repels water, and the weight of the displaced water exceeds that of the sample. As a result, it floats around for a few weeks.

Table 1 Water contact angle values after tape-peeling experiments for coated aluminium surfaces

	Water contact angle values (°)		
Cycles	Dodecanoic acid based coating	Octadecanoic acid based coating	Tetradecanoic acid based coating
0	168 ± 2	157 ± 2	165 ± 3
1	158 ± 3.25	155 ± 2.34	162 ± 2.34
2	156 ± 2.25	153 ± 1.87	159 ± 2.53
3	154 ± 2.30	150 ± 1.67	157 ± 1.98
4	151 ± 2.51	147 ± 1.29	155 ± 1.23
5	148 ± 3.12	143 ± 1.45	150 ± 1.29
10	138 ± 1.79	132 ± 2	145 ± 1.57
15	120 ± 2.13	125 ± 1.5	128 ± 1.22
20	110 ± 1.49	115 ± 1.45	120 ± 1.59

A water jet impact test was performed to examine the mechanical stability of the coated surfaces. When the water jet impacts the uncoated aluminium surface with a velocity of 6.5 ms^{-1}, water simply accumulates on the surface due to its hydrophilic nature.[31] However, the water jet bounced back when the coated surface was impinged with the water jet at an angle of 45° as shown in Fig. 6c. Water was continuously impacted for 2 min without any disturbance, and it was noticed that water bounced back from all three coated samples. This occurred because of higher water repellency (WCA ~158 ± 2°) and low tilt angle (TA ~7 ± 3°) even after water jet impact. Thus, it can be concluded that all surfaces showed the best mechanical durability of coatings. This observation was observed for all coated samples.

In day-to-day life or the industrial use of aluminium, there is a high chance of scratching while using it. For example, kitchen utensils are generally washed using polyethylene or metallic scrubbers; in this situation, there is a high chance of coating loss. Therefore, sandpaper abrasion tests were performed to evaluate the adhesion strength of the coatings on the substrates. For this, the sample was mounted on the surface of a 0.2 N weight and moved in the back-and-forth direction on the surface of 180 grit sandpaper as shown in Fig. 7a. The contact angles were measured after each cycle for the first five cycles, followed by angle measurement after every five cycles. The contact angles were measured at three different locations on the samples after the abrasion test to obtain their mean values, as shown in Table 2. The graph of the relationship between the WCA and abrasion test cycles is plotted as shown in Fig. 7b. There was a sudden decrease in the contact angle for the dodecanoic acid-coated surface where the angle decreased to 143 ± 2° after the 5th cycle. The octadecanoic acid-fabricated surface retained superhydrophobicity up to the 10th cycle, where the contact

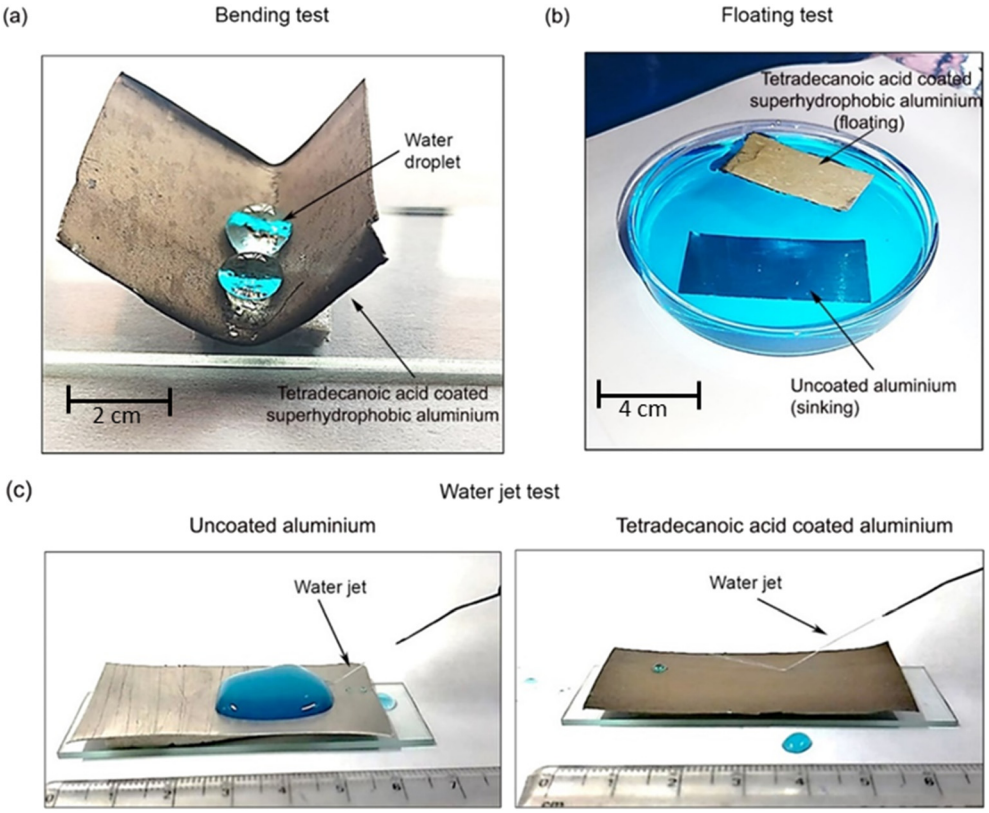

Fig. 6 Optical image of (a) water droplets on the V-shaped kink during the bending test, (b) tetradecanoic acid coated aluminium floating on the surface of the water while uncoated aluminium sank to the bottom, and (c) the water jet impact test on the tetradecanoic acid coated surface for the uncoated and coated samples.

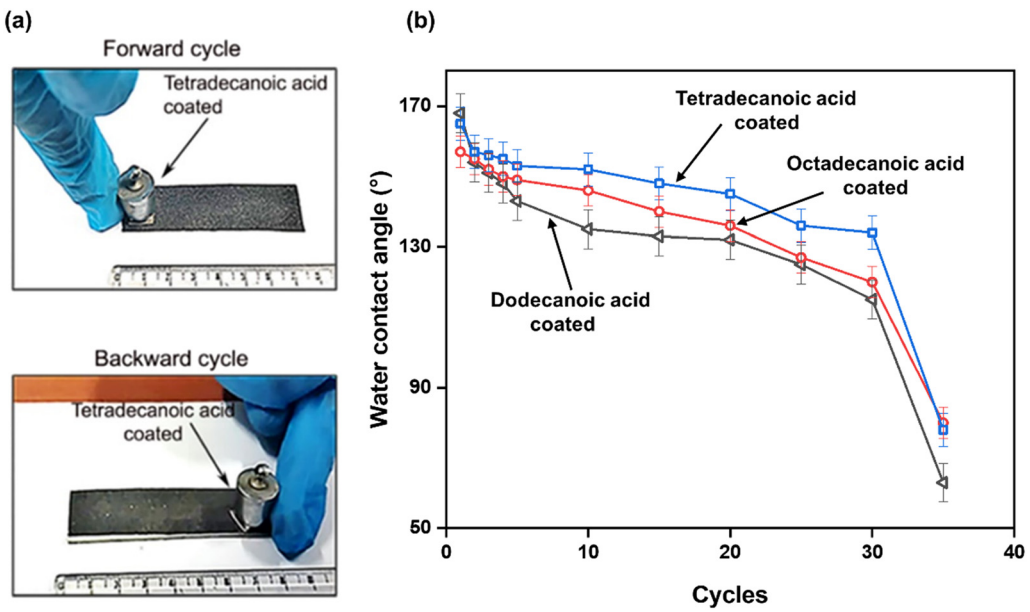

Fig. 7 (a) Optical images of the sandpaper abrasion test for examining the durability of the coating and (b) WCA *vs.* sandpaper abrasion cycle plot for coated surfaces.

angle was 146 ± 1°. The tetradecanoic acid coating was the most stable, and superhydrophobicity was lost after the 15th cycle of abrasion. The water contact angle is measured to be 148 ± 3°. After repeated cycles of applying mechanical stress to the surface, the coating or roughness may be lost due to the attack of the sharp edge of the sand particles of

Table 2 Water contact angle values after sandpaper abrasion experiments for coated aluminium surfaces

	Water contact angle values (°)		
Cycles	Dodecanoic acid based coating	Octadecanoic acid based coating	Tetradecanoic acid based coating
1	168 ± 2.22	157 ± 1.47	165 ± 1.12
2	154 ± 1.29	155 ± 1.25	157 ± 1.32
3	151 ± 1.29	152 ± 1.29	156 ± 2.26
4	148 ± 2.5	150 ± 2.12	155 ± 2.36
5	143 ± 1.43	149 ± 1.79	153 ± 1.25
10	135 ± 2.13	146 ± 1.43	152 ± 2.39
15	133 ± 1.22	140 ± 1.25	148 ± 2.42
20	132 ± 1.23	136 ± 1.34	145 ± 2.15
25	125 ± 1.82	127 ± 1.89	136 ± 1.26
30	115 ± 1.67	120 ± 1.44	134 ± 1.35
35	63 ± 1.31	80 ± 1.29	78 ± 1.45

sandpaper over coated surfaces, this leads to the loss of superhydrophobicity. Similar observations were reported by Tudu *et al.*[13]

The tendency is to produce a thin liquid film on metal surfaces in the presence of high salinity and acidity, which accelerates up the electrochemical corrosion of metals. To determine the chemical stability of the coated surface, the samples were immersed in solutions with different pH levels (pH 2, 3, 7, 8, 11, and 13).[32] The water contact angle was measured at a regular time interval of immersion until complete superhydrophobicity was lost. In the pH 2 solution, the dodecanoic acid-coated surface lost superhydrophobicity within 4 min of immersion whereas the octadecanoic and tetradecanoic acid-coated samples retained superhydrophobicity for 6 and 8 min, respectively, and the surface became completely worn out and stretches were observed. In the pH 2 solution, the concentration of H^+ ions is high, therefore there is a higher chance of etching or corrosion on the sample. These corrosive ions penetrate into the pores of the coating and react with the aluminium substrate, leading to the peeling of the coating material. Therefore, the coatings were completely unstable in extremely corrosive environments. A similar scenario can be seen in a highly basic medium (pH 11 and pH 13 solutions), which peels off the coating immediately due to the high concentration of OH^- ions. At pH 7 and mildly corrosive environments such as pH 8, the coatings were stable for 25 days and 3 days, respectively. Under these mild acidic and basic conditions, there is a very low concentration of H^+ or OH^- ions that are unable to penetrate into the coating, leaving the metal surfaces undamaged. The contact angles of the surfaces were found to be greater than 150° in mildly acidic and alkaline environments. Fig. 8a shows the comparison between the chemical stabilities of the molecules with different chain lengths in various pH solutions. It can be inferred that the coating is completely unstable in corrosive media, such as acids and alkalis, where the coatings react with them and lead to a damaged surface.

Materials must meet a certain threshold of temperature in order to be used. Sometimes aluminium is exposed to high temperatures, therefore the chance of damage to the coating is high. Therefore, it is necessary to determine the thermal stability of the coated samples to examine the performance of the coating at high temperatures. In this test, the samples were annealed at different temperatures ranging from 50 to 300 °C as shown in Fig. 8b. The samples were first annealed at a particular temperature for a period of 2 h and then subsequently cooled and the water contact angle was measured.[33] The contact angles were measured at three different locations in all samples to calculate their mean

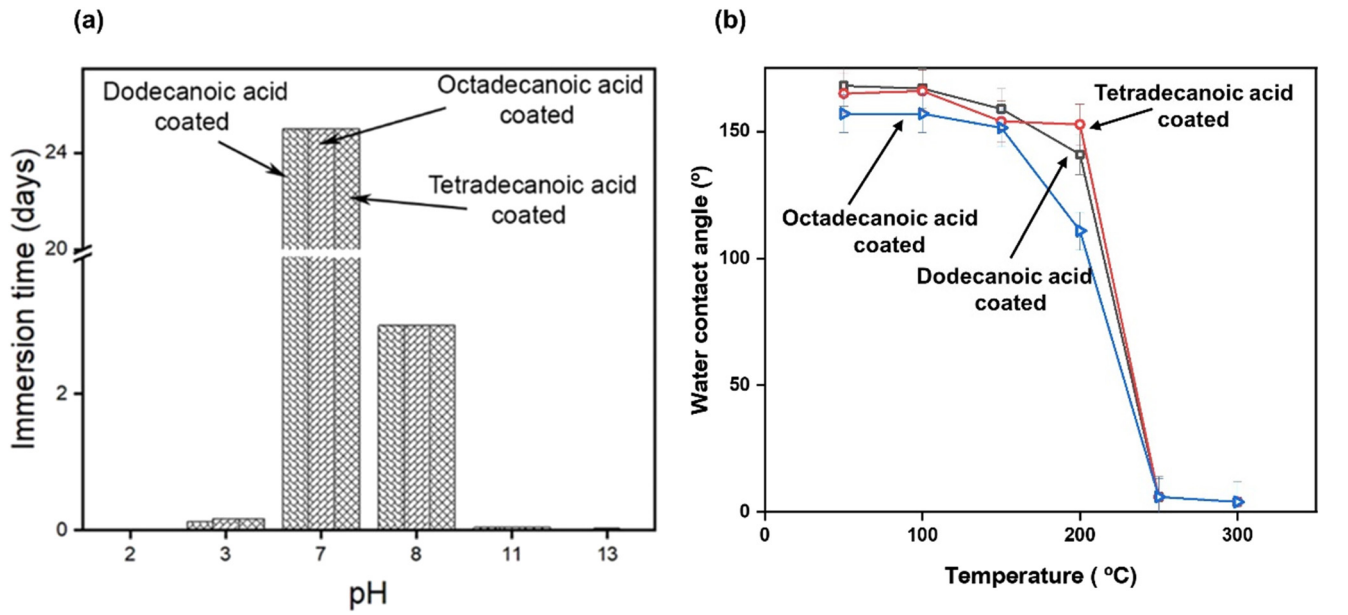

Fig. 8 (a) Samples immersed in solutions of varying pH levels retained their superhydrophobicity, demonstrating good chemical stability. (b) Water contact angle *vs.* temperature plot for all coated aluminium after 2 h of annealing, showing thermal stability of the coated samples.

Table 3 Water contact angle values after annealing the coated samples at different temperatures

Annealing temperature (°C)	Water contact angle values (°)		
	Dodecanoic acid based coating	Tetradecanoic acid based coating	Octadecanoic acid based coating
50	168 ± 2.25	165 ± 2.68	157 ± 2.58
100	167 ± 2.23	166 ± 2.75	157 ± 2.26
150	158.9 ± 1.89	154 ± 2.13	151.5 ± 2.78
200	141 ± 1.25	152.8 ± 1.97	110.8 ± 1.28
250	6 ± 0.47	6 ± 0.5	6 ± 0.57
300	4 ± 0.38	4 ± 0.32	4 ± 0.29

values as reported in Table 3. It can be seen that there are minute changes in the contact angle for the tetradecanoic acid up to 200 °C and superhydrophobicity was still retained. On the other hand, dodecanoic and octadecanoic acid-coated samples were superhydrophobic up to 150 °C but lost complete superhydrophobicity at 200 °C. Upon further increasing the temperature above 200 °C decompositions of different long-chain molecules take place due to the low melting point of these fatty acids and the surface becomes completely hydrophilic. No spherical droplets were observed while measuring the contact angle and the water completely wets the surfaces, when the samples were subjected to 250 °C and 300 °C.

3.3 Self-cleaning and corrosion resistance performance

Aluminium may occasionally have to deal with a dusty environment, which degrades the surface's functionality. Therefore, it should be cleaned by washing with detergent water, mechanically by rubbing or scrubbing, chemically using sanitizers, or by other chemicals such as acetone and vacuum cleaning. However, all of these conventional cleaning methods have their own limitations; for example, mechanical scrubbing can change surface properties. Similarly, detergent washing and chemical treatments can be used on a small scale and are not applicable everywhere. So, the self-cleaning properties of the coated and uncoated aluminium were inspected by dropping water droplets on the chalk and dust-sprinkled surfaces. Fig. 9 shows the self-cleaning behavior of the uncoated and coated samples. The dust particles stick to the water droplets and are easily removed from all the coated surfaces. On the uncoated surface, the water completely spreads and sticks to the dust particles and the surface in contact. Therefore, it did not exhibit self-cleaning characteristics. The adhesion forces between the superhydrophobic surface and dust particles were very low, which attributed to their excellent self-cleaning behavior. In this way, the surface was completely cleaned. Similar observations were observed for all three coated samples.

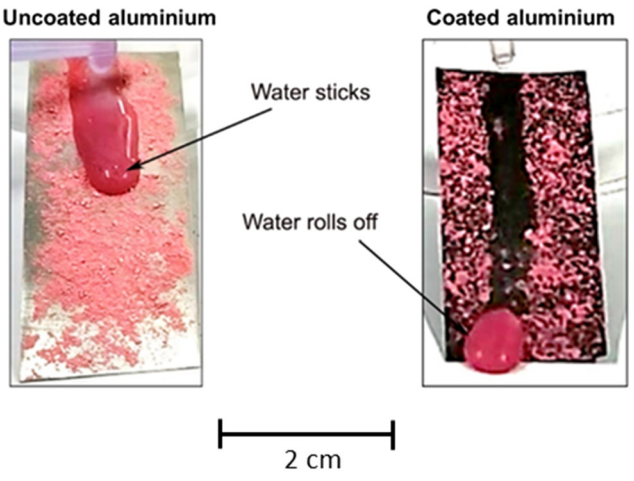

Fig. 9 Optical images showing the self-cleaning behavior of uncoated and tetradecanoic acid-coated aluminum surfaces. Dust particles remain adhered to the uncoated surface, whereas water droplets roll off the coated surface with effectively removing the dust and demonstrating the self-cleaning effect.

Due to the presence of an inherent native oxide layer that stops the oxidation of the surface, aluminium maintains its corrosion resistance in the air. However, it experiences corrosion under continuous moisture contact. Corrosion makes it susceptible to more damage and causes the system to collapse permanently. Since the coating is an excellent water-repellent, it is expected that it would show corrosion resistance. To inspect the corrosion behavior of the superhydrophobic coating on the aluminium surface, the potentiodynamic polarization test was performed. In this work, the samples were immersed in NaCl solution (3.5 wt%) for about 30 min, and with the help of a potentiostat, the value of E_{corr}, I_{corr}, anodic slope (β_a), cathodic slope (β_c), corrosion rate (CR) and polarisation resistance (R_p) for the uncoated and all different long-chain fatty acid coated surfaces are listed in Table 4. The value of I_{corr} is used to estimate the corrosion rate (CR) according to the equation:

$$\text{Corrosion rate (mm per year)} = \frac{0.00327 \times I_{corr} \times M}{nd} \quad (6)$$

M refers to the atomic mass of metal in (g mol^{-1}), n is the number of electrons involved in the oxidation of metal during the process of corrosion, I_{corr} is corrosion current density in A cm^{-2} and d is the density of the metal in (g cm^{-3}). The anodic slope (β_a in mV dec^{-1}) and cathodic slope (β_c in mV dec^{-1}) on the Tafel plot are used to calculate the polarisation resistance (R_p in Ω cm^{-2}) using the Stern Geary equation:

Table 4 Corrosion data obtained from the Tafel plot for uncoated and different long-chain fatty acids coated aluminium surfaces

Samples	E_{corr}/V (*vs.* Ag/AgCl)	I_{corr} (A cm^{-2})	$-\beta_c$ (mV dec^{-1})	β_a (mV dec^{-2})	CR (mm per year)	R_p (Ω cm^{-2})
Uncoated	−0.8401	8.18×10^{-4}	312.36	121.79	8.9162	46.57
Dodecanoic acid based coating	−0.8167	4.22×10^{-5}	448.78	278.48	0.4599	1770.50
Tetradecanoic acid based coating	−0.7925	4.30×10^{-6}	287.98	152.33	0.0469	10 073.79
Octadecanoic acid based coating	−0.7819	1.48×10^{-6}	200.54	288.00	0.0161	34 729.92

$$R_p = \frac{\beta_a \times \beta_c}{2.3\, I_{corr}\, (\beta_a + \beta_c)} \quad (7)$$

The potentiodynamic polarization curve was obtained as shown in Fig. 10. The corrosion voltage E_{corr} is found to be −0.8401 V for the uncoated aluminium surface whereas for the coated surfaces the E_{corr} shifts towards a more positive value by an increment of 0.234 V, 0.0476 V, and 0.0582 V for dodecanoic acid, tetradecanoic acid, and octadecanoic acid coated surfaces, respectively. The corrosion current density value for uncoated aluminium is 8.18×10^{-4} A cm^{-2} which is 94.84%, 99.47%, and 99.81% higher than the I_{corr} observed for dodecanoic acid, tetradecanoic acid, and octadecanoic acid coated surfaces, respectively. The presence of a morphological layer on the aluminium surface hinders the attack of electrolytic corrosive species due to the water-repellent nature of the coated surfaces, which retards the corrosion rate compared with uncoated aluminium. The E_{corr} value for octadecanoic acid was −0.7819 V, which is the highest among all the samples and has the lowest corrosion current density of 1.48×10^{-6} A cm^{-2}. The increase in the corrosion inhibition potential of coated aluminium on increasing the size of alkyl chains is attributed to the fact that longer hydrocarbon chain provides much better packing, due to hydrophobic interaction among them, at the interface of the metal and electrolyte.[34] This makes the octadecanoic acid-coated sample the most resistant to corrosion in comparison to the other two superhydrophobic surfaces. So, the results signify that with the increase in the length of the carbon chain, the corrosion inhibition property also increases.

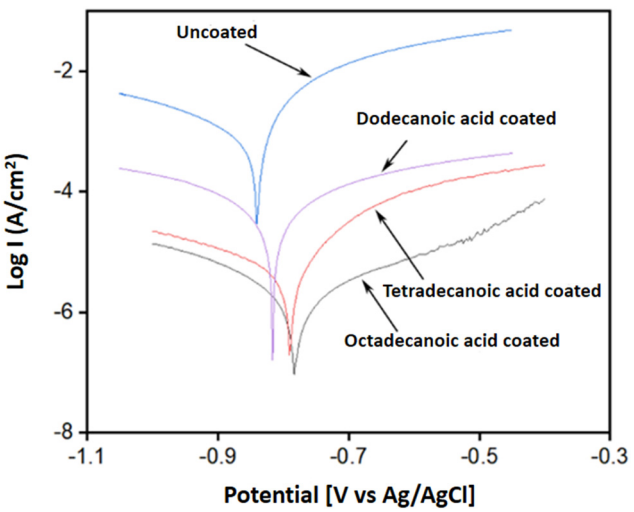

Fig. 10 Potentiodynamic polarization curves for uncoated and different long-chain fatty acid coated superhydrophobic aluminium surfaces in 3.5% (w/v) NaCl solution.

Better water resistance, durability, and corrosion resistance were displayed by fatty acids. Octadecanoic acid, which has a longer chain than dodecanoic and tetradecanoic acids, has more durability and resistance to corrosion and water than any other fatty acids. From the results above, the number of carbons in fatty acids directly relates to their corrosion resistance. In terms of production, the cost for water-repellent coatings on an industrial scale involves the use of intricate instrumentation and expensive materials such as silanes and polymers. However, among all the low surface energy materials, long-chain fatty acids are the most economical and efficient materials that can be fabricated by a simple immersion method. The estimated cost to produce the dodecanoic acid-coated aluminium surface is approximated to be 0.97 $ per m^2. However, the cost comes to around 0.98 $ per m^2 and 0.96 $ per m^2 for tetradecanoic and octadecanoic acid-coated aluminium substrates, respectively. Future research on other metals such as brass, zinc, and steel is possible because of the great results of the long-chain fatty acids in terms of water repellence, durability, and corrosion resistance.

4. Conclusions

In this study, superhydrophobic surfaces were developed by etching with NaOH followed by treatment with three different long carbon chain fatty acids (dodecanoic, tetradecanoic, and octadecanoic acid) *via* a simple immersion technique. Wettability and surface morphology were analysed using contact angle measurement and SEM, respectively. A static water contact angle of 168 ± 2° after modification with dodecanoic acid, 165 ± 3° after modification with tetradecanoic acid, and 157 ± 2° after modification with octadecanoic acid was found. The presence of methyl and ethyl group peaks in FTIR plots confirmed the presence of long-chain fatty acids in the coating. Additionally, the mechanical durability was inspected using tape peeling, abrasion, and water jet impact tests. In the tape peeling test, superhydrophobicity losses after the 5th cycle, 10th cycle, and 3rd cycle in the case of dodecanoic, tetradecanoic, and octadecanoic acid-coated samples, respectively. In the bending test, it is observed that superhydrophobicity remains unaltered for up to 15 cycles in the case of the dodecanoic acid-coated sample. Whereas in the case of tetradecanoic and

octadecanoic acid-coated samples, it is up to 17 and 20 cycles, respectively. In the abrasion test, superhydrophobicity is lost for the dodecanoic, octadecanoic, and tetradecanoic acid-coated samples after the 5th cycle, 10th cycle, and 15th cycle of abrasion, respectively. The water jet impact and flotation tests show that all the surfaces exhibited excellent water repellency. In the thermal stability check, the dodecanoic and octadecanoic acid-coated samples remained unchanged up to 150 °C. Whereas, the coating of tetradecanoic acid retains superhydrophobicity up to 200 °C. All the coatings exhibit good chemical stability and superhydrophobicity in the mild acidic and alkaline environments. Furthermore, the coatings demonstrate excellent self-cleaning behavior, which makes them suitable for various industrial applications. Anticorrosion properties were examined using a potentiodynamic polarization test. It shows octadecanoic acid has excellent corrosion resistance among all those fatty acids. Based on the results for aluminum modified with three different long-chain fatty acids, it can be concluded that, in addition to the number of carbon atoms, overall performance, including coating durability (mechanical, chemical, and thermal) and corrosion resistance, depends not only on the chain length but also on the packing density of the fatty acids.

Data availability

The data supporting this article have been included as part of the ESI.†

Conflicts of interest

There are no conflicts to declare.

Acknowledgements

The authors are indebted to the Department of Science and Technology, Government of India (Grant No. DST/TDT/SHRI-32/2021(G)) for the financial support. The authors are also indebted to Dr. Balraj K. Tudu for his valuable help during the experiment.

References

1 W. Liu, S. Wang, G. Wang, J. Zhang and C. Zhou, Investigation on the differences of surface cleaning properties of series of superhydrophobic aluminium alloys, *Colloids Surf., A*, 2022, **651**, 129614, DOI: **10.1016/j.colsurfa.2022.129614**.

2 P. Rodic, B. Kapun and I. Milosev, Superhydrophobic aluminium surface to enhance corrosion resistance and obtain self-cleaning and anti-Icing ability, *Molecules*, 2022, **27**, 1099, DOI: **10.3390/molecules27031099**.

3 O. R. Ayra, A. B. Tahcheiva and N. L. Isern, Removal of dyes, oils, alcohols, heavy metals and microplastics from water with superhydrophobic materials, *Chemosphere*, 2022, **311**, 137148, DOI: **10.1016/j.chemosphere.2022.137148**.

4 S. K. Pandit, B. K. Tudu, I. M. Mishra and A. Kumar, Development of stain resistant, superhydrophobic and self-cleaning coating on wood surface, *Prog. Org. Coat.*, 2020, **139**, 105453, DOI: **10.1016/j.porgcoat.2019.105453**.

5 P. Chauhan, A. Kumar and B. Bhushan, Self-cleaning, stain-resistant and anti-bacterial superhydrophobic cotton fabric prepared by simple immersion technique, *J. Colloid Interface Sci.*, 2019, **535**, 66–74, DOI: **10.1016/j.jcis.2018.09.087**.

6 A. Kumar and M. K. Meena, Fabrication of durable corrosion-resistant polyurethane/SiO2 nanoparticle composite coating on aluminium, *Colloid Polym. Sci.*, 2021, **299**, 915–924, DOI: **10.1007/s00396-021-04814-9**.

7 A. Kumar and B. Gogoi, Development of durable self-cleaning superhydrophobic coatings for aluminium surfaces via chemical etching method, *Tribol. Int.*, 2018, **118**, 114–118, DOI: **10.1016/j.triboint.2018.02.032**.

8 A. K. Singh, Surface engineering using PDMS and functionalized nanoparticles for superhydrophobic coatings: Selective liquid repellence and tackling COVID-19, *Prog. Org. Coat.*, 2022, **171**, 107061, DOI: **10.1016/j.porgcoat.2022.107061**.

9 P. Walker and W. H. Tarn, *Handbook of metal etchant*, CRC Press, Washington, 1991.

10 D. Cumming, *Handbook of lithography*, Read Books, London, 2012.

11 T. S. Gick, *Etching, and other glass treatment*, Gick Publishing Inc., New York, 1980.

12 B. Redwood, F. Schoffer and B. Garret, *The 3-D printing handbook*, 3D Hubs, Chicago, 2017.

13 B. K. Tudu, A. Kumar and B. Bhushan, Facile approach to develop anti-corrosive superhydrophobic aluminium with high mechanical, chemical and thermal durability, *Philos. Trans. R. Soc., A*, 2019, **377**, 1471–2962, DOI: **10.1098/rsta.2018.0272**.

14 H. Wang, D. Gao, Y. Meng, H. Wang, E. Wang and Y. Zhu, Corrosion-resistance, robust and wear-durable highly amphiphilic polymer based composite coating via a simple spraying approach, *Prog. Org. Coat.*, 2015, **82**, 74–80, DOI: **10.1016/j.porgcoat.2015.01.012**.

15 C. Chen, S. Yang, L. Liu, H. Xie, H. Liu, L. Zhu and X. Xu, A green one-step fabrication of superhydrophobic metallic surfaces of aluminium and zinc, *J. Alloys Compd.*, 2017, **711**, 506–513, DOI: **10.1016/j.jallcom.2017.04.050**.

16 P. Varshney, S. S. Mohapatra and A. Kumar, Superhydrophobic coatings for aluminium surfaces synthesized by chemical etching process, *Int. J. Smart Nano Mater.*, 2016, **7**, 248–264, DOI: **10.1080/19475411.2016.1272502**.

17 T. P. Rasitha, D. Nanda, G. Krishna, C. Thinaharan, S. C. Vanithakumari and J. Philip, Optimization of coating parameters for fabrication of robust superhydrophobic (SHP) aluminum and evaluation of corrosion performance in aggressive medium, *Prog. Org. Coat.*, 2022, **172**, 107076, DOI: **10.1016/j.porgcoat.2022.107076**.

18 H. Peng, L. Li, Q. Wang, Y. Zhang, T. Wang, B. Zheng and H. Zhou, Organic carbon dot coating for superhydrophobic

aluminium alloy surfaces, *J. Coat. Technol. Res.*, 2021, **18**, 861–869, DOI: **10.1007/s11998-020-00449-7**.

19 L. V. Shuwei, X. Zhang, X. Yang, X. Li, Z. Yang and Y. Zhai, Fabrication of superhydrophobic surface with corrosion resistance via cyclic chemical etching process on aluminum substrate, *Mater. Res. Express*, 2022, **9**, 026520, DOI: **10.1088/2053-1591/ac433a**.

20 Y. Zhang, J. Wu, X. Yu and H. Wu, Low-cost one step fabrication of superhydrophobic surface on Al alloy, *Appl. Surf. Sci.*, 2011, **257**, 7928–7931, DOI: **10.1016/j.apsusc.2011.03.096**.

21 P. Rodic, B. Kapun, M. Panjan and I. Milosev, Easy and fast fabrication of self-cleaning and anti-icing perfluoroalkyl silane film on aluminium, *Coatings*, 2020, **10**, 6–9, DOI: **10.3390/coatings10030234**.

22 L. Feng, H. Zhang, Z. Wang and Y. Liu, Superhydrophobic aluminum alloy surface: Fabrication, structure, and corrosion resistance, *Colloids Surf., A*, 2014, **441**, 319–325, DOI: **10.1016/j.colsurfa.2013.09.014**.

23 J. A. Budny, *Encyclopedia of Toxicology*, Academic Press, Imprint of Elsevier, Berkeley, 2014.

24 J. H. Chang and E. C. Pyo, Effects of Hydrophobic Modification of Linear- and Branch-Structured Fluorinated and Nonfluorinated Silanes on Mesoporous Silica Particles, *ACS Omega*, 2022, **7**, 26661–26669, DOI: **10.1021/acsomega.2c02918**.

25 S. Bharathala and P. Sharma, *Biomedical Applications of Nanoparticles. Nanotechnology in Modern Animal Biotechnology*, Elsevier Inc., New York, 2018, pp. 113–132.

26 J. Lomga, P. Varshney, D. Nanda, M. Satapathy, S. S. Mohapatra and A. Kumar, Fabrication of durable and regenerable superhydrophobic coatings with excellent self-cleaning and anti-fogging properties for aluminium surface, *J. Alloys Compd.*, 2017, **702**, 161–170, DOI: **10.1016/j.jallcom.2017.01.243**.

27 P. Varshney, S. S. Mohapatra and A. Kumar, Superhydrophobic coatings for aluminium surfaces synthesized by chemical etching process, *Int. J. Smart Nano Mater.*, 2016, **7**, 248–264, DOI: **10.1080/19475411.2016.1272502**.

28 Y. Lei, H. Lan, B. Jiang, Y. Yuan, D. A. Vorontsov, G. Gao, Y. Zhang and Q. Chen, TiN/acetylene black composite coatings: Enhanced durability and superhydrophobicity for all-day anti-icing applications, *Appl. Surf. Sci.*, 2025, **680**, 161305, DOI: **10.1016/j.apsusc.2024.161305**.

29 B. Jiang, Y. Lei, H. Sui, J. Cao, G. Ye and Y. Yuan, Facile fabrication of a robust photothermal/electrothermal superhydrophobic coating for all-weather anti-icing/de-icing applications, *Prog. Org. Coat.*, 2025, **200**, 109085, DOI: **10.1016/j.porgcoat.2025.109085**.

30 H. O. S. Yadav, A.-T. Kuo, S. Urata and W. Shinoda, Effects of packing density and chain length on the surface hydrophobicity of thin films composed of perfluoroalkyl acrylate chains: A molecular dynamics study, *Langmuir*, 2019, **35**(43), 14316–14323, DOI: **10.1021/acs.langmuir.9b02656**.

31 S. Mohammad and R. Ardekani, Ultrasonic atomization based fabrication of superhydrophobic and corrosion-resistant hydrolyzed MTMS/PVDF coatings, *JCIS Open.*, 2022, **7**, 100059, DOI: **10.1016/j.jciso.2022.100059**.

32 H. Zhang, W. Sun, L. Wang, J. Wang, S. Wang and G. Liu, A mechanically and chemically stable superhydrophobic coating for preventing marine atmospheric corrosion, *Surf. Interfaces*, 2021, **27**, 101537, DOI: **10.1016/j.surfin.2021.101537**.

33 J. Shang, Y. Jiang and W. Wang, Heat stability and icing delay on superhydrophobic coatings in facile one step, *Polymers*, 2022, **14**(15), 3124, DOI: **10.3390/polym14153124**.

34 C. Verma, M. A. Quraishi and K. Y. Rhee, Hydrophilicity and hydrophobicity consideration of organic surfactant compounds: Effect of alkyl chain length on corrosion protection, *Adv. Colloid Interface Sci.*, 2022, **306**, 102723, DOI: **10.1016/j.cis.2022.102723**.